2009 IEEE/ASME International Conference on Advanced Intelligent Mechatronics
Suntec Convention and Exhibition Center
Singapore, July 14-17, 2009

Analysis of Inverse Kinematics and Dynamics of a Novel 6-Degree-of–freedom Wire-Driven Parallel Gantry Crane Robot

Ya-Qing ZHENG, Qi LIN，Jian-Po WU, Peter MITROUCHEV

***Abstract*—Every type of wire-driven parallel robots can be used in cargo handling as a robot crane. Concerning the 6-degree-of–freedom (DOF) wire-driven parallel robot with three wires, its mechanism configuration belongs to URPMs (Under Restrained Positioning Mechanisms), if one translational or rotational DOF rigid mechanism is added to each of its kinematic chains. In this case the mechanism becomes a new type 6-DOF robot. It has been found, in the research survey that the mechanism configuration of such kind of 6-DOF robot CABLEV is not powerful enough because of its limited workspace. A novel 6-DOF parallel crane robot containing three rigid-and-flexible hybrid sub-chains is proposed which can access to a larger workspace. The differential flatness of its inverse kinematics and dynamics is analyzed by a simulation. The results of this simulation will lay a basis for the future trajectory tracking control of the payload.**

I. Introduction

Wire-driven parallel robots are characterised by simple structure, low inertia, large workspace and high speed. According to the relationship between the number of wires m and the number of degrees of freedom (DOFs) of the end-effector n, wire-driven parallel robots can be classified into the following four types [1] : *i*) Incompletely Restrained Positioning Mechanisms (IRPMs), with $m=n$; *ii*) Completely Restrained Positioning Mechanisms (CRPMs), with $m=1+n$; *iii*) Redundantly Restrained Positioning Mechanisms (RRPMs), with $m>1+n$ and *iv*) Under Restrained Positioning Mechanisms (URPMs), with $m<n$.

All of these four types of wire-driven parallel robots can be introduced to crane technology as the concept of wire-driven parallel crane robot. Because the payload of the crane robot usually moves in a three dimensional space with three translational and three rotational independent motions, the concept of 6-DOF wire-driven parallel crane robot is addressed in this paper. In fact, such a RoboCrane belongs to IRPMs [2].

Manuscript received January 15, 2009. This work was supported in part by the National Natural Science Foundation of China (NSFC) under Grant 50805054.

Y. Q. Zheng is currently a postdoctor in the Department of Aeronautics, Xiamen University, Xiamen, 361005, China as well as working in College of Mechanical Engineering and Automation, Huaqiao University, 362021, China (e-mail: yq_zheng@ hqu.edu.cn).

Q. Lin is with the Department of Aeronautics, Xiamen University, Xiamen, 361005, China (corresponding author: 86-592-8968519; e-mail: qilin@xmu.edu.cn).

J. P. WU is currently with College of Mechanical Engineering and Automation, Huaqiao University, 362021, China(e-mail: topjianpo@ hqu.edu.cn).

P. MITROUCHEV is with Lab. G-SCOP, UMR 5272 CNRS, France (e-mail:Peter.Mitrouchev@g-scop.inpg.fr)

The 6-DOF wire-driven parallel robot driven by seven wires proposed by Kino Hithoshi belongs to RRPMs [3]. The 6-DOF wire-driven parallel crane robot proposed by Kleinschnittger belongs to RRPMs [4, 5]. The 6-DOF wire-driven parallel crane robot with three wires proposed by LIU Shuqing belongs to URPMs [6]. Let us note that in [6], it is wrong to assume that the robot is a 3-DOF manipulator because the end-effector is a 3-dimensional solid which is connected by three wires via three point-shaped joints.

The four kinds of 6-DOF wire-driven crane robots mentioned above have their own special applications in practice. Till now, the mechanism theory and control technology for the first three kinds of them are mature and there are a lot of literature and prototypes for reference, so there is a promising future for their application.

Concerning the fourth kind of wire-driven parallel robot, its application is limited because of the property of being under-constrained. In 1992, Arai presented a 6-DOF hybrid crane robot by adding a three DOFs (two Translational DOFs and one Rotational DOF) strut serial robot into it [7]. Thus, the robot is able to lift a heavier payload than the classic cranes and has a weak stiffness because of its hybrid structure. Inverse kinematics and kinematic control of the hybrid robot have been presented in [8, 9] for a deeper understanding of this robot.

Instead, since 1998, a new kind of crane robot, CABLEV, is proposed by adding a translational DOF rigid mechanism into each kinematic chain of the fourth kind of robot, in which the three rigid mechanisms are in parallel [10]. The flatness of the CABLEV system is analyzed and the trajectory tracking of the payload based on differential flatness is carried out in the prototype [11]. Yamamoto Motoji has presented another similar kind of 6-DOF crane robot by implementing a feedback linearization control scheme in a prototype [12]. The authors call the two kinds of robots mentioned above as “6-DOF under-restrained wire-driven parallel crane robot with three wires” [13]. However, the three rails of the CABLEV system are in parallel, so three wire coordinates should satisfy four equations for describing the problem of its generalized inverse kinematics, with the result that the trajectory of the payload is limited and the volume of the workspace cannot fill the total space of the base. In order to overcome the disadvantage of the limited workspace, a new 6-DOF wire-driven parallel crane robot is proposed here, in which two parallel rails are vertical to the third one. Inverse systems based on differential flatness are analyzed and a simulation is given under the environment of Matlab, which will lay on foundation for the further trajectory tracking of the payload.

II. MECHANISM CONFIGURATION OF A 6-DOF WIRE-DRIVEN PARALLEL CRANE ROBOT

The mechanism configuration of the presented novel 6-DOF wire-driven parallel crane robot with three wires is shown in Fig.1 (a).The base is composed of two landing legs and three rails, and each trolley moves along its corresponding rail by a girder. Each of the three capstans is mounted on the frame of every trolley, which will drive its own wire to handle the payload in three dimensional space in order to realize 6-DOF motions. In the real cargo-handling trajectory, the three trolleys are moving along their own rails and the three wires actuated by the winches change their lengths to make the payload realize its desired trajectory.

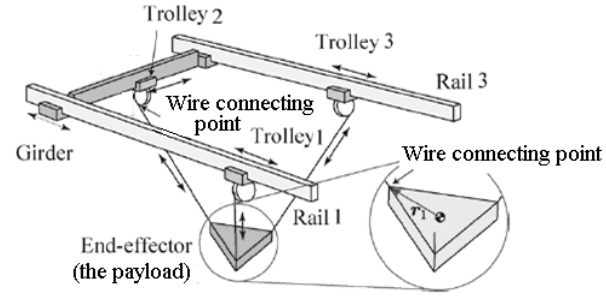

(a) mechanism configuration

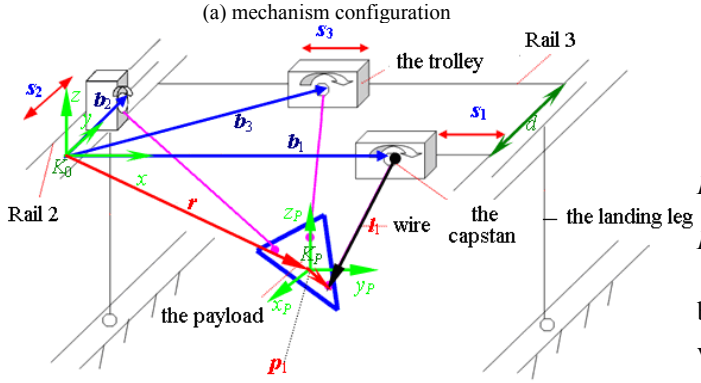

(b) geometric parameters

Fig.1: Mechanism sketch of the 6-DOF wire-driven parallel crane robot with 3 wires

As shown in Fig.1(b), the independently controllable robot coordinates of the actuators can be expressed: $\boldsymbol{q}=(s_1 \quad s_2 \quad s_3 \quad l_1 \quad l_2 \quad l_3)^{\mathrm{T}} \in R^6$, the vector of the three trolley coordinates is $\boldsymbol{q}_1=(s_1 \quad s_2 \quad s_3)^{\mathrm{T}}$, and the vector of the wire length is $\boldsymbol{q}_2=(l_1 \quad l_2 \quad l_3)^{\mathrm{T}}$.The posture of the reference point P of the payload is $\boldsymbol{y}_P=\begin{pmatrix}\boldsymbol{r}\\ \boldsymbol{\alpha}\end{pmatrix}$, here, $\boldsymbol{r}=(r_x \quad r_y \quad r_z)^{\mathrm{T}}$ and $\boldsymbol{\alpha}=(\varphi_1 \quad \varphi_2 \quad \varphi_3)^{\mathrm{T}}$. The position vector of the reference point P of the payload in the fixed coordinate system K_0 is $\boldsymbol{r}$ and the orientation vector $\boldsymbol{\alpha}$ is the vector of three Cardan angles of the payload in the moving coordinate system, K_P, corresponding to fixed coordinate system , K_0. The 1st rail is parallel to the 3rd one (rail), the distance between which is d, and both of them are parallel to the 2nd rail.

III. MODELLING OF THE 6-DOF WIRE-DRIVEN PARALLEL CRANE ROBOT

A. Coordinate Systems of the Actuators and the Payload

The payload should realize 6-DOF motions in the real handling task, the posture of which can not be determined by the length of three wires, so it is necessary to solve the problem of generalized inverse kinematics of the robots to determine the length of the three wires and the positions of the three trolleys.

The velocity vector of the reference point P of the payload in the fixed coordinate system K_0 is $\dot{\boldsymbol{s}}_P=\begin{pmatrix}\boldsymbol{v}\\ \boldsymbol{\omega}\end{pmatrix}$, here $\boldsymbol{v}=\dot{\boldsymbol{r}}=\begin{pmatrix}\dot{r}_x & \dot{r}_y & \dot{r}_z\end{pmatrix}^{\mathrm{T}}$ is the translational velocity vector, $\boldsymbol{\omega}=(\omega_x \quad \omega_y \quad \omega_z)^{\mathrm{T}}$ is the vector of angular velocity of the reference point P of the payload in the fixed coordinate system K_0 .The derivatives of the posture vector $\boldsymbol{y}_P$ corresponding to time, t, is $\dot{\boldsymbol{y}}_P=\boldsymbol{H}(\boldsymbol{y}_P)\dot{\boldsymbol{s}}_P$, in detail, it is $\begin{pmatrix}\dot{\boldsymbol{r}}\\ \dot{\boldsymbol{\alpha}}\end{pmatrix}=\begin{bmatrix}\boldsymbol{I}_{3\times3} & \boldsymbol{0}\\ \boldsymbol{0} & \boldsymbol{H}_{\omega}(\boldsymbol{\alpha})\end{bmatrix}\begin{pmatrix}\boldsymbol{v}\\ \boldsymbol{\omega}\end{pmatrix}$, and $\boldsymbol{H}_{\omega}(\boldsymbol{\alpha})=$

$$\frac{1}{\cos\varphi_2}\begin{bmatrix}\cos\varphi_2 & \sin\varphi_1\sin\varphi_2 & -\cos\varphi_1\sin\varphi_2\\ 0 & \cos\varphi_1\cos\varphi_2 & \sin\varphi_1\cos\varphi_2\\ 0 & -\sin\varphi_1 & \cos\varphi_1\end{bmatrix}.$$

B. Constraint Equations

B.1 Geometric constraints on position level

According to Fig.1, the geometric constraints equations between the coordinates of the actuators $\boldsymbol{q}$ and the posture vector $\boldsymbol{y}_P$, are as follows:

$$\boldsymbol{g}_i(\boldsymbol{q};\boldsymbol{y}_P)=\boldsymbol{l}_i^{\mathrm{T}}\boldsymbol{l}_i-\|\boldsymbol{l}_i\|^2=\boldsymbol{0} \tag{1}$$

The wire vector $\boldsymbol{l}_i(\boldsymbol{q};\boldsymbol{y}_P)$ in the fixed coordinate system K_0 can be expressed by the following equation:

$$\boldsymbol{l}_i=\boldsymbol{r}+{}^P\boldsymbol{T}(\boldsymbol{\alpha})\,{}^P\boldsymbol{p}_i-\boldsymbol{b}_i\ (i=1,2,3) \tag{2}$$

The above three vectors are as follows:

$\boldsymbol{l}_1=\boldsymbol{r}+{}^P\boldsymbol{T}(\boldsymbol{\alpha})\,{}^P\boldsymbol{p}_1-(s_1 \quad 0 \quad 0)^{\mathrm{T}}$, $\boldsymbol{l}_2=\boldsymbol{r}+{}^P\boldsymbol{T}(\boldsymbol{\alpha})\,{}^P\boldsymbol{p}_2-(0 \quad s_2 \quad 0)^{\mathrm{T}}$, $\boldsymbol{l}_3=\boldsymbol{r}+{}^P\boldsymbol{T}(\boldsymbol{\alpha})\,{}^P\boldsymbol{p}_2-(0 \quad d \quad 0)^{\mathrm{T}}-(s_3 \quad 0 \quad 0)^{\mathrm{T}}$.

Vectors $\boldsymbol{p}_i\ (i=1,2,3)$ are three constant vectors of the payload in the moving coordinate system K_P, here: ${}^P\boldsymbol{p}_1=(\sqrt{3}/3l \quad 0 \quad 0)^{\mathrm{T}}$, ${}^P\boldsymbol{p}_2=(-\sqrt{3}/6l \quad -l/2 \quad 0)^{\mathrm{T}}$, ${}^P\boldsymbol{p}_3=(-\sqrt{3}/6l \quad l/2 \quad 0)^{\mathrm{T}}$.

Vector ${}^P\boldsymbol{T}(\boldsymbol{\alpha})$ is the transformation matrix between the fixed coordinate system K_0 and the moving coordinate system, K_P, which satisfies:

$$\boldsymbol{T}(\boldsymbol{\alpha})=\boldsymbol{T}_z(\varphi_3)\boldsymbol{T}_y(\varphi_2)\boldsymbol{T}_x(\varphi_1)=\begin{bmatrix}\cos\varphi_3 & -\sin\varphi_3 & 0\\ \sin\varphi_3 & \cos\varphi_3 & 0\\ 0 & 0 & 1\end{bmatrix}$$

$$\begin{bmatrix}\cos\varphi_2 & 0 & \sin\varphi_2\\ 0 & 1 & 0\\ -\sin\varphi_2 & 0 & \cos\varphi_2\end{bmatrix}\begin{bmatrix}1 & 0 & 0\\ 0 & \cos\varphi_1 & -\sin\varphi_1\\ 0 & \sin\varphi_1 & \cos\varphi_1\end{bmatrix}$$. So the following expressions can be obtained:

$$\boldsymbol{l}_1=\begin{pmatrix} r_x+\frac{\sqrt{3}}{3}l\cos\varphi_2\cos\varphi_3-s_1\\ r_y-\frac{\sqrt{3}}{3}l\cos\varphi_2\sin\varphi_3\\ r_z-\frac{\sqrt{3}}{3}l\sin\varphi_2\cos\varphi_3\end{pmatrix},$$

$$\boldsymbol{l}_2=\begin{pmatrix} r_x-\frac{\sqrt{3}}{6}l\cos\varphi_2\cos\varphi_3-\frac{1}{2}l(\sin\varphi_1\sin\varphi_2\cos\varphi_3\\ -\cos\varphi_1\sin\varphi_3)\\ r_y-\frac{\sqrt{3}}{6}l\cos\varphi_2\sin\varphi_3-\frac{1}{2}l(\sin\varphi_1\sin\varphi_2\sin\varphi_3\\ +\cos\varphi_1\cos\varphi_3)-s_2\\ r_z+\frac{\sqrt{3}}{6}l\sin\varphi_2-\frac{1}{2}l\sin\varphi_1\cos\varphi_2\end{pmatrix},$$

$$\boldsymbol{l}_3=\begin{pmatrix} r_x-\frac{\sqrt{3}}{6}l\cos\varphi_2\cos\varphi_3+\frac{1}{2}l(\sin\varphi_1\sin\varphi_2\cos\varphi_3\\ -\cos\varphi_1\sin\varphi_3)-s_3\\ r_y-\frac{\sqrt{3}}{6}l\cos\varphi_2\sin\varphi_3+\frac{1}{2}l(\sin\varphi_1\sin\varphi_2\sin\varphi_3\\ +\cos\varphi_1\cos\varphi_3)-d\\ r_z+\frac{\sqrt{3}}{6}l\sin\varphi_2+\frac{1}{2}l\sin\varphi_1\cos\varphi_2\end{pmatrix}.$$

B.2 Constraints on velocity level

The derivatives of the vectors of the length of three wires in Eq. (2) corresponding to time, t, can be shown in the following equations:

$$\begin{aligned}\dot{\boldsymbol{l}}_1&=\dot{\boldsymbol{r}}+\dot{\boldsymbol{p}}_1-\begin{pmatrix}\dot{s}_1 & 0 & 0\end{pmatrix}^{\mathrm{T}}\\ \dot{\boldsymbol{l}}_2&=\dot{\boldsymbol{r}}+\dot{\boldsymbol{p}}_2-\begin{pmatrix}0 & \dot{s}_2 & 0\end{pmatrix}^{\mathrm{T}}\\ \dot{\boldsymbol{l}}_3&=\dot{\boldsymbol{r}}+\dot{\boldsymbol{p}}_3-\begin{pmatrix}\dot{s}_3 & 0 & 0\end{pmatrix}^{\mathrm{T}}\end{aligned}\tag{3}$$

The derivatives of the vector of wire length in Eq.(1) corresponding to time, t, can be shown in the following equations:

$$\dot{\boldsymbol{g}}_i=2\boldsymbol{l}_i^{\mathrm{T}}\dot{\boldsymbol{l}}_i-2\|\boldsymbol{l}_i\|\dot{\boldsymbol{l}}_i=0\ (i=1,2,3)\tag{4}$$

The derivatives of $\boldsymbol{p}_i\ (i=1,2,3)$ corresponding to time, t, can be expressed as the following equations:

$$\dot{\boldsymbol{p}}_i=\tilde{\boldsymbol{\omega}}\boldsymbol{p}_i,\quad \tilde{\boldsymbol{\omega}}=\begin{bmatrix}0 & -\omega_z & \omega_y\\ \omega_z & 0 & -\omega_x\\ -\omega_y & \omega_x & 0\end{bmatrix}=-\tilde{\boldsymbol{\omega}}^{\mathrm{T}}\tag{5}$$

Here, $\tilde{\boldsymbol{\omega}}\boldsymbol{p}_i=\boldsymbol{\omega}\times\boldsymbol{p}_i$, $\dot{\boldsymbol{l}}_i=\dot{\boldsymbol{r}}+\dot{\boldsymbol{p}}_i-\dot{\boldsymbol{b}}_i=\boldsymbol{v}+\tilde{\boldsymbol{\omega}}\boldsymbol{p}_i-\dot{\boldsymbol{b}}_i$ (6)

In detail, $\dot{\boldsymbol{l}}_1=\begin{pmatrix}v_x-\dot{s}_1\\ v_y+\frac{\sqrt{3}}{3}l\omega_z\\ v_z-\frac{\sqrt{3}}{3}l\omega_y\end{pmatrix}$, $\dot{\boldsymbol{l}}_2=\begin{pmatrix}v_x-\dot{s}_2+\frac{1}{2}l\omega_z\\ v_y-\frac{\sqrt{3}}{6}l\omega_z\\ v_z-\frac{l}{2}\omega_x+\frac{\sqrt{3}}{6}l\omega_y\end{pmatrix}$,

$\dot{\boldsymbol{l}}_3=\begin{pmatrix}v_x-\dot{s}_3-\frac{1}{2}l\omega_z\\ v_y-\frac{\sqrt{3}}{6}l\omega_z\\ v_z+\frac{l}{2}\omega_x+\frac{\sqrt{3}}{6}l\omega_y\end{pmatrix}$, $\dot{\boldsymbol{q}}_2=\begin{pmatrix}\dot{l}_1=\|\dot{\boldsymbol{l}}_1\|\\ \dot{l}_2=\|\dot{\boldsymbol{l}}_2\|\\ \dot{l}_3=\|\dot{\boldsymbol{l}}_3\|\end{pmatrix}$.

According to Eqs. (3), (4) and (5), we can obtain:

$$\dot{\boldsymbol{g}}\equiv\boldsymbol{G}_s(\boldsymbol{q}_1;\boldsymbol{y}_P)\dot{\boldsymbol{s}}_P+\boldsymbol{G}_q(\boldsymbol{q};\boldsymbol{y}_P)\dot{\boldsymbol{q}}=\boldsymbol{0}\tag{7}$$

The constraint matrix $\boldsymbol{G}_s(\boldsymbol{q}_1;\boldsymbol{y}_P)$ satisfies:

$$\boldsymbol{G}_s(\boldsymbol{q}_1;\boldsymbol{y}_P)=\begin{bmatrix}2\boldsymbol{l}_1^{\mathrm{T}} & -2\boldsymbol{l}_1^{\mathrm{T}}\tilde{\boldsymbol{p}}_1\\ 2\boldsymbol{l}_2^{\mathrm{T}} & -2\boldsymbol{l}_2^{\mathrm{T}}\tilde{\boldsymbol{p}}_2\\ 2\boldsymbol{l}_3^{\mathrm{T}} & -2\boldsymbol{l}_3^{\mathrm{T}}\tilde{\boldsymbol{p}}_3\end{bmatrix}=\begin{bmatrix}\boldsymbol{G}_{\mathrm{T}} & \boldsymbol{G}_{\mathrm{R}}\end{bmatrix}\in\mathrm{R}^{3\times6}\tag{8}$$

Here, $\dot{\boldsymbol{l}}_1=\begin{pmatrix}l_{1x}\\ l_{1y}\\ l_{1z}\end{pmatrix}$, $\dot{\boldsymbol{l}}_2=\begin{pmatrix}l_{2x}\\ l_{2y}\\ l_{2z}\end{pmatrix}$, $\dot{\boldsymbol{l}}_3=\begin{pmatrix}l_{3x}\\ l_{3y}\\ l_{3z}\end{pmatrix}$.

Also we can obtain the following equation:

$$\boldsymbol{G}_q(\boldsymbol{q};\boldsymbol{y}_P)=-2\begin{bmatrix}\boldsymbol{l}_1^{\mathrm{T}}\boldsymbol{e}_x & 0 & 0 & l_1 & 0 & 0\\ 0 & \boldsymbol{l}_2^{\mathrm{T}}\boldsymbol{e}_x & 0 & 0 & l_2 & 0\\ 0 & 0 & \boldsymbol{l}_3^{\mathrm{T}}\boldsymbol{e}_x & 0 & 0 & l_3\end{bmatrix}\tag{9}$$

Here, $\boldsymbol{e}_x=\begin{bmatrix}1 & 0 & 0\end{bmatrix}^{\mathrm{T}}$, $\boldsymbol{l}_i^{\mathrm{T}}(i=1,2,3)\in\mathrm{R}^{1\times3}$,

$\boldsymbol{G}_q(\boldsymbol{q};\boldsymbol{y}_P)=-2\begin{bmatrix}l_{1x} & 0 & 0 & l_1 & 0 & 0\\ 0 & l_{2x} & 0 & 0 & l_2 & 0\\ 0 & 0 & l_{3x} & 0 & 0 & l_3\end{bmatrix}\in\mathrm{R}^{3\times6}$.

Because of $\dot{\boldsymbol{q}}=-(\boldsymbol{G}_q)^{+}(\boldsymbol{G}_s\dot{\boldsymbol{s}}_P)$, we can obtain $\dot{\boldsymbol{q}}_1=\begin{pmatrix}\dot{s}_1 & \dot{s}_2 & \dot{s}_3\end{pmatrix}^{\mathrm{T}}$ and $\dot{\boldsymbol{q}}_2=\begin{pmatrix}\dot{l}_1 & \dot{l}_2 & \dot{l}_3\end{pmatrix}^{\mathrm{T}}$.

B.3 Constraints on the acceleration level

The derivatives of Eq.(7) corresponding to time, t, can be shown in the following equation:

$$\ddot{\boldsymbol{g}}\equiv\boldsymbol{G}_s(\boldsymbol{q}_1;\boldsymbol{y}_P)\ddot{\boldsymbol{s}}_P+\boldsymbol{G}_q(\boldsymbol{q};\boldsymbol{y}_P)\ddot{\boldsymbol{q}}+\dot{\boldsymbol{G}}_s\dot{\boldsymbol{s}}_P+\dot{\boldsymbol{G}}_q\dot{\boldsymbol{q}}=\boldsymbol{0}\tag{10}$$

Here, $\boldsymbol{\gamma}(y_P,\boldsymbol{q},\dot{\boldsymbol{s}}_P,\dot{\boldsymbol{q}})=\dot{\boldsymbol{G}}_s\dot{\boldsymbol{s}}_P+\dot{\boldsymbol{G}}_q\dot{\boldsymbol{q}}$.

C. Dynamic Equation

C.1 Dynamic equation of the payload using $\boldsymbol{y}_P$, $\dot{\boldsymbol{s}}_P$ and $\ddot{\boldsymbol{s}}_P$

The dynamic equation of the payload can be expressed by the following 6 equations:

$$\begin{bmatrix} m\boldsymbol{I} & \boldsymbol{0} \\ \boldsymbol{0} & \boldsymbol{\theta}_P \end{bmatrix}_{6\times 6}\begin{pmatrix} \dot{\boldsymbol{v}} \\ \dot{\boldsymbol{\omega}} \end{pmatrix}+\begin{pmatrix} \tilde{\boldsymbol{\omega}} & \boldsymbol{o} \\ \boldsymbol{\omega}(\boldsymbol{\theta}_{\mathrm{p}}\boldsymbol{\omega}) \end{pmatrix}=\begin{pmatrix} \boldsymbol{F}_{\mathrm{G}} \\ 0 \end{pmatrix}+\begin{pmatrix} \boldsymbol{G}_{\mathrm{T}}^{\mathrm{T}} \\ \boldsymbol{G}_{\mathrm{R}}^{\mathrm{T}} \end{pmatrix}_{6\times 3}\begin{pmatrix} \lambda_1 \\ \lambda_2 \\ \lambda_3 \end{pmatrix} \tag{11}$$

It can be expressed as $\boldsymbol{M}_s\ddot{\boldsymbol{s}}_P+\boldsymbol{k}_s=\boldsymbol{W}_{\mathrm{G}}+\boldsymbol{G}_s^{\mathrm{T}}\boldsymbol{\lambda}$ in matrix form，here m is the mass of the payload, $\boldsymbol{\theta}_{\mathrm{P}}$ is the inertia tensor of the payload corresponding to the moving coordinate system K_P，$\boldsymbol{F}_{\mathrm{G}}$ is the gravity vector of the payload，$\boldsymbol{\lambda}\in R^{3\times 1}$，the Lagrange multiply, stands for the coordinates of the wire tensions，and the vector of tension of three wires can be expressed by: $\boldsymbol{F}_i=2\boldsymbol{l}_i^T\lambda_i\,(i=1,2,3)$.

C.2 Dynamic equations of the actuators

The dynamic equations of the actuators composed by the three trolleys and the capstans are as follows:

$$\boldsymbol{M}_q\ddot{\boldsymbol{q}}=\boldsymbol{B}_q\boldsymbol{u}+\boldsymbol{G}_q^{\mathrm{T}}\boldsymbol{\lambda} \tag{12}$$

Here，$\boldsymbol{q}$ is the vector of the actuators accelerations，$\boldsymbol{M}_q$ is the mass matrix of the actuators, i.e.,

$$\boldsymbol{M}_q=\begin{bmatrix} m_{\mathrm{k}} & 0 & 0 & 0 & 0 & 0 \\ 0 & m_{\mathrm{k}} & 0 & 0 & 0 & 0 \\ 0 & 0 & m_{\mathrm{k}} & 0 & 0 & 0 \\ 0 & 0 & 0 & \dfrac{J}{r^2} & 0 & 0 \\ 0 & 0 & 0 & 0 & \dfrac{J}{r^2} & 0 \\ 0 & 0 & 0 & 0 & 0 & \dfrac{J}{r^2} \end{bmatrix}\in \mathrm{R}^{6\times 6}$$

, m_{k} is the mass of the trolley, J is the inertia of the capstan, and r is the radius of the capstan.

$$\boldsymbol{B}_q=\begin{bmatrix} 1 & 0 & 0 & 0 & 0 & 0 \\ 0 & 1 & 0 & 0 & 0 & 0 \\ 0 & 0 & 1 & 0 & 0 & 0 \\ 0 & 0 & 0 & \dfrac{1}{r} & 0 & 0 \\ 0 & 0 & 0 & 0 & \dfrac{1}{r} & 0 \\ 0 & 0 & 0 & 0 & 0 & \dfrac{1}{r} \end{bmatrix}\in \mathrm{R}^{6\times 6},\quad \boldsymbol{u}=\begin{pmatrix} u_{s1} \\ u_{s2} \\ u_{s3} \\ u_{l1} \\ u_{l2} \\ u_{l3} \end{pmatrix}\in \mathrm{R}^{6\times 1}$$

, here $u_{si}(i=1,2,3)$ is the driving forces of the trolleys and $u_{li}(i=1,2,3)$ the torques driving the capstans. $\boldsymbol{G}_q^{\mathrm{T}}$ can be seen in Eq.(9)，$\boldsymbol{\lambda}$ can be obtained from Eq. (11)，and $\ddot{\boldsymbol{q}}$ can be obtained from Eq. (10)，thus the expression of the vector $\boldsymbol{u}$ can be obtained as follows: $\boldsymbol{u}=(\boldsymbol{B}_q)^{-1}(\boldsymbol{M}_q\ddot{\boldsymbol{q}}-\boldsymbol{G}_q^{\mathrm{T}}\boldsymbol{\lambda})$.

IV. THE DIFFERENTIAL FLATNESS OF THE 6-DOF WIRE-DRIVEN PARALLEL CRANE ROBOT

A. The Problem of Generalized Inverse Pose Kinematics

A.1 On the position level

The problem of generalized inverse position kinematics of the robots can be described as the determination of the vector $\boldsymbol{q}(t)$ when the vector of the desired posture $\boldsymbol{y}_P(t)$ is given. There are only three equations for determination of the length of the three wires, so there needs three additional equations.

The vector of the reference point P, $\boldsymbol{s}_P(t)$ and its velocity vector $\dot{\boldsymbol{s}}_P(t)$ can be obtained from the vector of $\boldsymbol{y}_P(t)$. And the payload is in the dynamic equilibrium along the trajectory, $\boldsymbol{y}_P(t)$, which can be expressed by:

$$\boldsymbol{G}_s^{\mathrm{T}}(\boldsymbol{q}_1;\boldsymbol{y}_P)\boldsymbol{\lambda}=-\boldsymbol{W}_{\mathrm{d}}(\boldsymbol{y}_P,\dot{\boldsymbol{s}}_P,\ddot{\boldsymbol{s}}_P) \tag{13}$$

Here,

$$\boldsymbol{W}_{\mathrm{d}}(\boldsymbol{y}_P,\dot{\boldsymbol{s}}_P,\ddot{\boldsymbol{s}}_P)=\boldsymbol{W}_{\mathrm{G}}-\boldsymbol{M}_s\ddot{\boldsymbol{s}}_P-\boldsymbol{K}_s \tag{14}$$

The components of the wire tension, $\boldsymbol{\lambda}$ can be calculated by the 3rd, 4th and 5th row of Eq. (10), i.e.,

$$\boldsymbol{\lambda}=\phi_\lambda(\boldsymbol{q}_1;\boldsymbol{y}_P) \tag{15}$$

If we insert Eq. (15) into the 1st, 2nd and 6th of Eq. (13), we can obtain $\boldsymbol{q}_1=\begin{pmatrix} s_1 & s_2 & s_3 \end{pmatrix}^{\mathrm{T}}$，and the vector of wire length $\boldsymbol{q}_2=\begin{pmatrix} l_1 & l_2 & l_3 \end{pmatrix}^{\mathrm{T}}$ can be obtained by $l_i=\|\boldsymbol{l}_i\|=\sqrt{\boldsymbol{l}_i^{\mathrm{T}}\boldsymbol{l}_i}$ $(i=1,2,3)$, so we can obtain the vector $\boldsymbol{q}$.

A.2 On the velocity level

The derivatives of Eq. (11) corresponding to time, t, can be shown in the following equation:

$$\boldsymbol{M}_s\boldsymbol{s}_P{}^{(3)}+\frac{\partial}{\partial\boldsymbol{y}_P}\boldsymbol{M}_s\boldsymbol{H}\dot{\boldsymbol{s}}_P\ddot{\boldsymbol{s}}_P+\frac{\partial}{\partial\boldsymbol{y}_P}\boldsymbol{H}(\boldsymbol{k}_s^c-\boldsymbol{k}_s^e)\dot{\boldsymbol{s}}_P+\frac{\partial}{\partial\dot{\boldsymbol{s}}_P}\boldsymbol{H}(\boldsymbol{k}_s^c-\boldsymbol{k}_s^e)$$

$$\ddot{\boldsymbol{s}}_P-(\frac{\partial}{\partial\boldsymbol{q}}\boldsymbol{G}_s^{\mathrm{T}}\boldsymbol{\lambda}\dot{\boldsymbol{q}}+\frac{\partial}{\partial\boldsymbol{y}_P}\boldsymbol{G}_s^{\mathrm{T}}\boldsymbol{H}\boldsymbol{\lambda}\dot{\boldsymbol{s}}_P)-\boldsymbol{G}_s^{\mathrm{T}}\dot{\boldsymbol{\lambda}}=\boldsymbol{0}$$

Then, one has:

$$\begin{bmatrix} \boldsymbol{L}_0 & \boldsymbol{G}_s^{\mathrm{T}} \\ \boldsymbol{G}_q & \boldsymbol{0} \end{bmatrix}\begin{bmatrix} \dot{\boldsymbol{q}} \\ \dot{\boldsymbol{\lambda}} \end{bmatrix}=\begin{bmatrix} \boldsymbol{M}_s\boldsymbol{s}_P{}^{(3)}+\boldsymbol{L}_2\ddot{\boldsymbol{s}}_P+\boldsymbol{L}_1\dot{\boldsymbol{s}}_P \\ -\boldsymbol{G}_s\dot{\boldsymbol{s}}_P \end{bmatrix} \tag{16}$$

Here,

$$\boldsymbol{L}_0=\frac{\partial\boldsymbol{G}_s^{\mathrm{T}}\boldsymbol{\lambda}}{\partial\boldsymbol{q}}\quad \boldsymbol{L}_1=\frac{\partial}{\partial\boldsymbol{y}_P}(\boldsymbol{M}_s\ddot{\boldsymbol{s}}_P+\boldsymbol{k}_s^c-\boldsymbol{k}_s^e-\boldsymbol{G}_s^{\mathrm{T}}\boldsymbol{\lambda})\boldsymbol{H},$$

$$\boldsymbol{L}_2=\frac{\partial}{\partial\dot{\boldsymbol{s}}_P}(\boldsymbol{k}_s^c-\boldsymbol{k}_s^e).$$

The vector $\dot{\boldsymbol{q}}$ can be obtained from Eq. (7), and if $\boldsymbol{\lambda}$ and $\dot{\boldsymbol{q}}$ are inserted into Eq. (16), $\dot{\boldsymbol{\lambda}}$ can be obtained. We can find that $\dot{\boldsymbol{q}}$ and $\dot{\boldsymbol{\lambda}}$ can be expressed by $\boldsymbol{y}_P$，$\dot{\boldsymbol{s}}_P$，$\ddot{\boldsymbol{s}}_P$ and $\boldsymbol{s}_P{}^{(3)}$.

A.3 On the acceleration level

From Eq. (10), we can obtain

$$\ddot{\boldsymbol{q}} = (\boldsymbol{G}_q)^{+}(-\dot{\boldsymbol{G}}_s \dot{\boldsymbol{s}}_P - \dot{\boldsymbol{G}}_q \dot{\boldsymbol{q}} - \boldsymbol{G}_s(\boldsymbol{q}_1; \boldsymbol{y}_P)\ddot{\boldsymbol{s}}_P) \tag{17}$$

The derivatives of Eq. (16) corresponding to time, t, can be expressed by Eq. (18), then if we insert Eq. (17) into Eq.(18) we can get the expression of $\ddot{\boldsymbol{\lambda}}$.

$$\boldsymbol{A}(\boldsymbol{y}_P, \boldsymbol{q}) \begin{bmatrix} \ddot{\boldsymbol{q}} \\ \ddot{\boldsymbol{\lambda}} \end{bmatrix} = \boldsymbol{b}(\boldsymbol{y}_P, \boldsymbol{s}_P, \dot{\boldsymbol{s}}_P, \ddot{\boldsymbol{s}}_P, \boldsymbol{s}_P^{(3)}, \boldsymbol{s}_P^{(4)}, \boldsymbol{q}, \dot{\boldsymbol{q}}) \tag{18}$$

Obviously, $\ddot{\boldsymbol{q}}$ and $\ddot{\boldsymbol{\lambda}}$ can be expressed by $\boldsymbol{y}_P$, $\dot{\boldsymbol{s}}_P$, $\ddot{\boldsymbol{s}}_P$, $\boldsymbol{s}_P^{(3)}$ and $\boldsymbol{s}_P^{(4)}$.

B. The solutions to dynamics equation

Given the condition is satisfied, i.e., $\boldsymbol{u} = (\boldsymbol{B}_q)^{-1}(\boldsymbol{M}_q \ddot{\boldsymbol{q}} - \boldsymbol{G}_q^{\mathrm{T}} \boldsymbol{\lambda})$, we can get the following equation:

$$\boldsymbol{u} = \boldsymbol{\varphi}_{\boldsymbol{u}}(\boldsymbol{y}_P, \boldsymbol{s}_P, \dot{\boldsymbol{s}}_P, \ddot{\boldsymbol{s}}_P, \boldsymbol{s}_P^{(3)}, \boldsymbol{s}_P^{(4)}) \tag{19}$$

The static variables $\boldsymbol{x} = [\boldsymbol{q}, \dot{\boldsymbol{q}}]^{\mathrm{T}} \in \mathrm{R}^{6\times 1}$ can be expressed by:

$$\boldsymbol{x} = \boldsymbol{\varphi}_x(\boldsymbol{y}_P, \boldsymbol{s}_P, \dot{\boldsymbol{s}}_P, \ddot{\boldsymbol{s}}_P, \boldsymbol{s}_P^{(3)}) \tag{20}$$

Given that the condition is satisfied, i.e., $\dot{\boldsymbol{s}}_P = \boldsymbol{H}^{-1}(\boldsymbol{y}_P)\dot{\boldsymbol{y}}_P$, we can obtain:

$$\boldsymbol{x} = \boldsymbol{\varphi}_x(\boldsymbol{y}_P, \dot{\boldsymbol{y}}_P, \ddot{\boldsymbol{y}}_P, \boldsymbol{y}_P^{(3)}) \tag{21}$$

$$\boldsymbol{u} = \boldsymbol{\varphi}_{\boldsymbol{u}}(\boldsymbol{y}_P, \dot{\boldsymbol{y}}_P, \ddot{\boldsymbol{y}}_P, \boldsymbol{y}_P^{(3)}, \boldsymbol{y}_P^{(4)}) \tag{22}$$

So the robot system is characterized by differential flatness on the basis of kinematic and dynamic levels. Simulation about this performance will be performed (made) in the next section.

V. SIMULATION

As shown in Fig. (1), the dimension of the robot system is as follows: d=5 m, m=0.5 Kg, l=0.1 m, $\boldsymbol{\theta}_{\mathrm{P}} =$

$$\begin{bmatrix} \frac{ml^2}{6} & 0 & 0 \\ 0 & \frac{ml^2}{6} & 0 \\ 0 & 0 & 0 \end{bmatrix}$$

, m_{k}=30 kg, J=0.06 Kg.m^2, r= 0.1 m.

Here we discuss the simulation of the solutions to the problems of inverse kinematics and dynamics when the payload moves along the z axis with pure translation. The problems can be described as follows:

Known: $\ddot{\boldsymbol{r}} = \begin{pmatrix} \ddot{r}_x = 0 & \ddot{r}_y = 0 & \ddot{r}_z = 0.1 \end{pmatrix}^{\mathrm{T}} \ (ms^{-2})$,

$\dot{\boldsymbol{r}} = \begin{pmatrix} \dot{r}_x = 0 & \dot{r}_y = 0 & \dot{r}_z = 0.1t \end{pmatrix}^{\mathrm{T}} \ (ms^{-1})$,

$\boldsymbol{r} = \begin{pmatrix} r_x = 0 & r_y = 0 & r_z = -6 + 0.05t^2 \end{pmatrix}^{\mathrm{T}} \ (m)$,

$\boldsymbol{\alpha} = \begin{pmatrix} \varphi_1 = 0 & \varphi_2 = 0 & \varphi_3 = 0 \end{pmatrix}^{\mathrm{T}}$,

$\boldsymbol{\omega} = \begin{pmatrix} \omega_x = 0 & \omega_y = 0 & \omega_z = 0 \end{pmatrix}^{\mathrm{T}}$,

$\boldsymbol{\varepsilon} = \begin{pmatrix} \dot{\omega}_x = 0 & \dot{\omega}_y = 0 & \dot{\omega}_z = 0 \end{pmatrix}^{\mathrm{T}}$, the curves of the vectors $\boldsymbol{q}$, $\dot{\boldsymbol{q}}$, $\ddot{\boldsymbol{q}}$ and $\boldsymbol{u}$ corresponding to t are ready to be calculated when t begins from 0 to 10 seconds. The curve of the vector, $\boldsymbol{F}_i = 2\boldsymbol{l}_i^T \lambda_i \ (i = 1,2,3)$, corresponding to t can be obtained as well.

According to the theoretical results presented in Section Ⅳ, a simulation under the environment of Matlab was performed. The results for these vectors are presented in Fig.2, Fig.3, Fig.4 , Fig.5, and Fig.6 respectively.

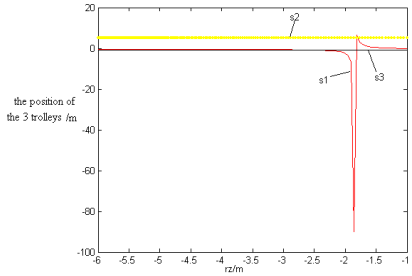

(a) s_1, s_2 and s_3 versus r_z

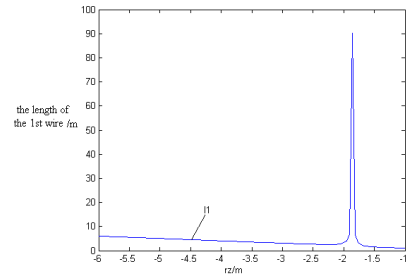

(b) l_1 versus r_z

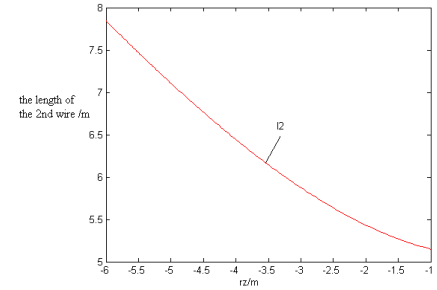

(c) l_2 versus r_z

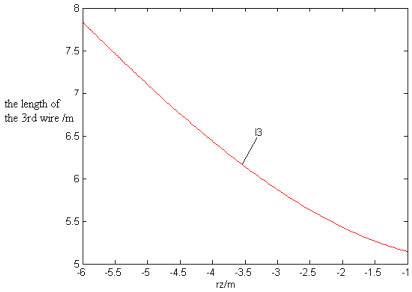

(d) l_3 versus r_z

Fig.2: $\boldsymbol{q}$ versus r_z

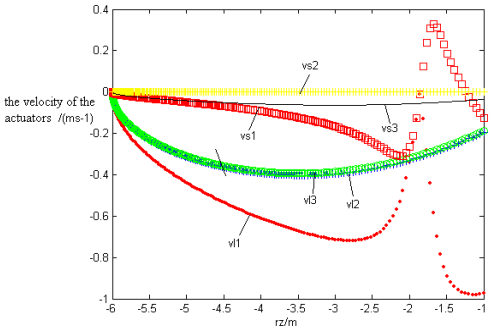

Fig.3: $\dot{\boldsymbol{q}}$ versus r_z

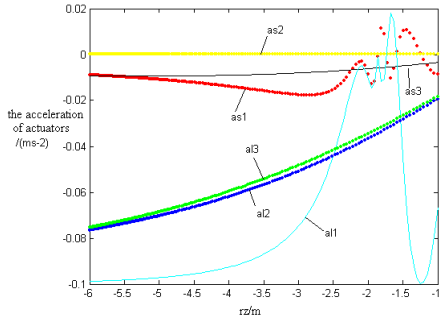

Fig.4: $\ddot{\boldsymbol{q}}_1$ and $\ddot{\boldsymbol{q}}_2$ versus r_z

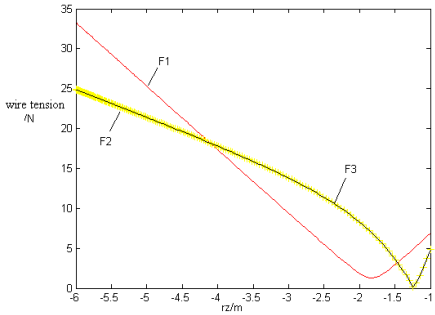

Fig.5: $\boldsymbol{F}$ versus r_z

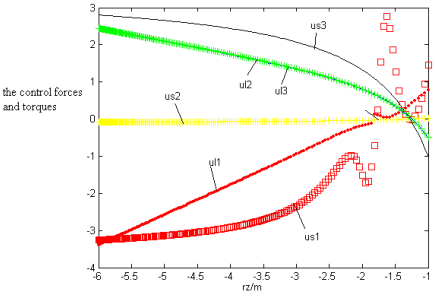

Fig.6: $\boldsymbol{u}$ versus r_z

From the simulation results, we can find that the values of position, velocity, acceleration and the control forces (torques) of the 1st trolley and the 1st wire are a bit large. It may be noted that the higher the payload moves, the larger variations are which may generate swing motions. Consequently an anti-swing control is necessary in the future design of the position controller of the payload. Concerning the issue of its stiffness and dynamic stability, it will be investigated in the further research using ANSYS software.

VI. CONCLUSIONS

(1) There are a lot of advantages for introducing the technology of wire-driven parallel robots into the automation of cranes, and different types of wire-driven parallel robots can satisfy different applications.

(2) A new 6-DOF wire-driven parallel crane robot is proposed, in which two parallel rails are vertical to the 3rd one, so that the workspace of the payload can fulfill the total volume of the base of the robot.

(3) Inverse kinematic and dynamic systems based on differential flatness of the robot have been analyzed. The simulation results have shown that the property is useful for trajectory generation, but the payload is easy to swing at high speed which should be considered in the future design of the position controller.

(4) Currently a prototype is being built in order to validate the simulation results presented above.

REFERENCES

[1] MING A, HIGUCHI T. Study on multiple degree of freedom positioning mechanisms using wires (Part 1): concept, design and control [J]. International Journal of the Japan Society for Precision Engineering, 1994, 28(2): 131-138.

[2] ALBUS J S, BOSTELMAN R V, DAGALAKIS N. The NIST ROBOCRANE [J]. Journal of Robotics System, 1992, 10 (5): 709-724.

[3] KINO H, YAHIRO T, TAKEMURA F, et al. Robust PD control using adaptive compensation for completely restrained parallel-wire driven robots: translational systems using the minimum number of wires under zero-gravity condition [J]. IEEE Transactions on Robotics, 2007, 23(4): 803-812.

[4] GENG Y F, CHEN F. Research of Position and Orientation Workspaces for Wire-Driven Parallel Crane Robot[J] Science & Technology Information , 2007,(20):28-29.

[5] ZHENG Y Q. A Wire-Driven Parallel Crane Robot for Containers Handling: Theory and Simulation [J]. Journal of Huaqiao University(Natural Science Edition)(in press)

[6] LIU S Q, WU H T. Kinematic Analysis and Application of a New Style Crane Robot [J].Journal of Hebei University of Science and Technology,2004,25(2):58-61.

[7] Arai T, Osumi H. Three Wire Suspension Robot. Industrial Robot, 1992(19):17-22.

[8] MAIER T, WOERNLE C. Inverse Kinematics for an Underconstrained Cable Suspension Manipulator[C]. Advances in Robot Kinematics: Analysis and Control, Kluwer Academic Publishers, Dordrecht, 1998: 97-104.

[9] MAIER T, WOERNLE C Kinematic Control of Cable Suspension Robots[C]. Proceedings of the NATO-ASI Computational Methods in Mechanisms, Varna, 1997, 2: 421-430.

[10] MAIER T, WOERNLE C. Flatness-based control of underconstrained cable suspension manipulators[C]. Proceedings of ASME Design Engineering Technical Conference, Las Vegas, NV,1999

[11] HEYDEN T, WOERNLE C. Dynamics and flatness-based undetermined cable suspension manipulator [J]. Multibody System Dynamics, 2006(16): 155–177.

[12] YAMAMOTO M, YANAI N, MOHRI A. Trajectory control of incompletely restrained parallel wire-suspended mechanism based on inverse dynamics[J]. IEEE transactions on robotics, 2004, 20(5): 840-850.

[13] ZHENG Y Q. Kinematics Control of a Large-Sized Wire-Driven Parallel Gantry Crane Robot for Shipyards [J]. Mechatronics Technology, 2007(S): 224-227.